Collagen has a unique SEC24 preference for efficient export from the endoplasmic reticulum

Chung-Ling Lu[1], Jacob Cain[2], Jon Brudvig[2], Steven Ortmeier[2], Simeon A. Boyadjiev[3], Jill M. Weimer[2], and Jinoh Kim[1,*]

[1]Department of Biomedical Sciences, College of Veterinary Medicine, Iowa State University, Ames, IA, 50011, USA

[2]Pediatrics and Rare Diseases Group, Sanford Research, Sioux Falls, SD, 57104, USA.

[3]Department of Pediatrics, University of California Davis School of Medicine, Sacramento, CA, 95817, USA

*To who correspondence should be addressed: Jinoh Kim, 2086 Vet Med, 1800 Christensen Drive, Iowa State University, Ames, IA 50011, Email: jinohk@iastate.edu, Tel: 515-294-3401

Key words: COPII; collagen; endoplasmic reticulum; SEC24; secretion; tissue-specificity

ABSTRACT

Procollagen requires COPII coat proteins for export from the endoplasmic reticulum (ER). SEC24 is the major component of the COPII proteins that selects cargo during COPII vesicle assembly. There are four paralogs (A to D) of SEC24 in mammals, which are classified into two subgroups. Pathological mutations in *SEC24D* cause osteogenesis imperfecta with craniofacial dysplasia in humans and *sec24d* mutant fish also recapitulate this phenotypes. Consistent with the skeletal phenotypes, the secretion of collagen was severely defective in mutant fish, emphasizing the importance of SEC24D in collagen secretion. However, SEC24D patient-derived fibroblasts show only a mild secretion phenotype, suggesting tissue-specificity in the secretion process. To explore this possibility, we generated *Sec24d* knockout (KO) mice. Homozygous KO mice died prior to bone development. When we analyzed embryonic and extraembryonic tissues of mutant animals, we observed tissue-dependent defects of procollagen processing and ER export. The spacial patterns of these defects mirrored with SEC24B deficiency. By systematically knocking down the expression of *Sec24* paralogs, we determined that, in addition to SEC24C and SEC24D, SEC24A and SEC24B also contribute to collagen secretion. In contrast, fibronectin 1 preferred either SEC24C or SEC24D. On the basis of our results, we propose that procollagen interacts with multiple SEC24 paralogs for efficient export from the ER, and that this is the basis for tissue-specific phenotypes resulting from SEC24 paralog deficiency.

INTRODUCTION

Collagens comprise about a third of the total protein in humans and are the major constituent of the extracellular matrix (ECM)(Shoulders and Raines, 2009). Collagens are synthesized as pre-procollagen in the endoplasmic reticulum (ER) and exit the ER as procollagen, which is rapidly processed to a mature form in the Golgi and in the extracellular space of animal tissues (Canty and Kadler, 2005; Shoulders and Raines, 2009). The exit of procollagen from the ER depends on the coat protein complex II (COPII) (Lu and Kim, 2020; McCaughey and Stephens, 2018). SEC24 proteins are COPII components that are mainly responsible for packaging cargo molecules into COPII vesicles (Zanetti et al., 2012). There are four SEC24 paralogs (SEC24A-D) in vertebrates and each SEC24 paralog has multiple cargo binding pockets, partly accounting for the ability of COPII to recognize diverse cargo molecules (Mancias and Goldberg, 2008; Miller et al., 2003; Mossessova et al., 2003). The SEC24 paralogs are classified into two subgroups based on their primary amino acid sequences and structures: one includes SEC24A and SEC24B, the other includes SEC24C and SEC24D. These two subgroups each display a shared and a distinctive cargo selectivity, mediated by selective binding of various transport signals on cargos and SNARE proteins (Adolf et al., 2016; Ma et al., 2017; Mancias and Goldberg, 2008).

SEC24 mutations tend to cause tissue-specific defects, depending on the nature of the mutation and on the organism. *Sec24a* knockout (KO) mice develop and live normally except that mutant animals exhibit markedly reduced plasma cholesterol levels due to defective ER export of PCSK9, a negative regulator of the low-density lipoprotein receptor (Chen et al., 2013). *Sec24b* deletion causes a completely open neural tube in mice, which occurs because VAGNL2 fails to be sorted into COPII vesicles (Merte et al., 2010). *Sec24c* disruption results in embryonic

lethality (Adams et al., 2014). Conditional knockout of *Sec24c* in neural progenitors during embryogenesis causes apoptotic cell death of post-mitotic neurons in the cerebral cortex (Wang et al., 2018). The neuronal cell death caused by *Sec24c* ablation was rescued in knock-in mice expressing *Sec24d* in place of *Sec24c*, which indicates a functional equivalency of SEC24C and SEC24D for this aspect (Wang et al., 2018). Compound heterozygous *SEC24D* mutations cause osteogenesis imperfecta with craniofacial dysplasia in humans (Garbes et al., 2015). In mice, homozygous *Sec24d* deletion ($Sec24d^{gt/gt}$, a gene-trap mutation) cause embryonic lethality near the 8-cell stage and hypomorphic *Sec24d* KO mutants ($Sec24d^{g2t/gt2}$) survive to mid-embryogenesis (embryonic day, E13.5) (Baines et al., 2013). Because of the early embryonic lethality, the role of SEC24D in skeletal formation remains unknown in mice. *sec24d* mutant fish display severe craniofacial and skeletal dysplasia (Ohisa et al., 2010; Sarmah et al., 2010). The cartilage cells of the *sec24d* mutant fish accumulate procollagen in the ER, which is consistent with the observed skeletal defects. *sec24c* morphants do not show craniofacial cartilage dysmorphology (Sarmah et al., 2010). However, craniofacial development in *sec24c;sec24d* double morphants arrested earlier than in *sec24d* single mutants, indicating that Sec24C has a partial role in chondrogenesis. Thus, among SEC24 paralogs, SEC24D is the most critical for skeletal formation both in humans and in zebrafish. These *in vivo* observations suggest that procollagens are predominatly recognized by SEC24D and to a lesser degree by SEC24C.

The severe bone fragility in patients carrying *SEC24D* mutations and the strong accumulation of procollagen in the ER in *sec24d* mutant fish predict that collagen secretion should be impaired in the human patients' cells. Skin fibroblasts derived from a SEC24D-deficient patient, however, displayed only a mild accumulation of collagen in the ER (Garbes et al., 2015). Thus, there seems to be other cellular factors that modulate the collagen secretion

phenotype in SEC24D-compromised cells and tissues. In this study, we present evidence that other SEC24 paralogs are the cellular factors compensating for the SEC24D deficiency.

RESULTS

The processing of procollagen depends on SEC24D and other factor(s)

To examine the involvement of SEC24D in collagen secretion, we generated *Sec24d*$^{gt2/gt2}$ mice as previously described (Baines et al., 2013). As the *Sec24d* knockout mice are embryonically lethal near E13.5 (prior to skeletal development) we decided to monitor collagen processing in embryonic tissues. Procollagen is proteolytically processed to collagen in post ER compartments as procollagen peptidases are present both in the Golgi and in the extracellular space (Fig. 1A) (Canty and Kadler, 2005). ER export inhibition imposed by *Sec23a* deletion results in pronounced ER accumulation of procollagen and an almost complete inhibition of the proteolytic processing of procollagen *in vivo* (Zhu et al., 2015). Thus, we anticipated consistent, similarly severe collagen phenotypes in the *Sec24d*$^{gt2/gt2}$ embryos. Surprisingly, however, the mutant embryos showed a variable and relatively modest processing defect of type I procollagen (COL1A1) (Fig. 1B, compare 36D with 36E). Interestingly, we observed a prominent inhibition of collagen processing to the mature form (Fig. 1C, see 92a and 92d) and occasionally aberrant processing (Fig. 1C, see 92a, open arrowhead) in the yolk sacs of *Sec24d* KO mice. These results suggest that SEC24D plays an important role in the ER export of procollagen, but that a tissue-dependent factor(s) influences the necessity for SEC24D.

Collagen accumulates in the ER of the yolk sac of Sec24d KO mice

We also performed immunohistochemistry on embryonic tissues to visualize COL1A distribution patterns and potential disruptions. Given the observed mild accumulation of collagen in the ER of skin fibroblasts from a SEC24D patient (Garbes et al., 2015), we examined COL1A signal in

the embryonic head skin. Wild-type and *Sec24d*$^{gt2/gt2}$ embryos had similar distribution of COL1A within head skin, with most fibroblasts displaying consistent punctate signal throughout the tissue and some deposition distal to superficial cells (Fig. 2A-D). Sporadic cells with more intense COL1A signal appeared in both genotypes.

When comparing patterns within the yolk sacs, however, striking differences were apparent. The inner mesoderm layer of the wild-type yolk sac has a high collagen content within the ECM (Carvalho et al., 2004). Wild-type tissues displayed diffuse COL1A signal throughout the yolk sac cells, with distinct, thin ECM deposits on the lumenal side of the inner mesoderm cells (Fig. 2E and F). *Sec24d*$^{gt2/gt2}$ yolk sacs lacked these deposits, instead displaying extensive intracellular accumulation (Fig. 2G and H). The lumenal mesoderm cells were distended and malformed, with COL1A deposits occupying a large portion of the cell body. We also examined the localization of another potential secretory cargo of the ECM, fibronectin 1 (FN1), in both tissues but did not observe any differences between genotypes (Fig. 2I-P). Together, these results support a cargo-specific, tissue-specific necessity for SEC24D in COL1A ER export.

The factor(s) affecting the tissue dependency is likely a component involved in ER export

An ER export block can enlarge ER cisternae. In particular, the ER accumulation of procollagen can contribute to ER enlargement as collagens are the most abundant secretory proteins (Shoulders and Raines, 2009). Thus, we expected to observe a significant ER distension in the tissues of *Sec24d* KO mice. Unexpectedly, however, almost no ER distension was observed in the cells of the head or the tail in the mutants (Fig. 1D). A significant ER distension was observed in the yolk sac in the mutants. These results are in line with our biochemical and

immunohistochemical results showing prominent collagen processing defects in the mutant yolk sacs. Importantly, this ER distention is not fully explained by a simple lack of SEC24D, as this phenotype is completely absent in skin fibroblasts. One possible explanation is that some tissues express another component of ER export machinery that is able to compensate for loss of SEC24D. Thus, we hypothesized that the severe phenotypes we observed in the yolk sac were caused by combined deficiencies in SEC24D and at least one other ER export protein that has low level or negligible expression in this tissue.

SEC24B and SEC24C are deficient in the wild-type yolk sacs

We suspected that the unknown tissue-specific compensatory factor(s) is a SEC24 paralog. For example, SEC24C is close to SEC24D in its amino acid sequence, 3D structure and cargo preference (Adolf et al., 2016; Ma et al., 2017; Mancias and Goldberg, 2008), but its expression level may differ in the embryo and the yolk sac. To test this possibility, we probed for the expression of *Sec24* paralogs in the extracts derived from embryos and yolk sacs (Fig. 3). We measured *Sec24a* transcript levels using a real-time quantitative PCR (RT-qPCR), because we were not able to obtain a reliable antibody specific for mouse SEC24A. *Sec24a* transcript levels were significantly higher in yolk sacs than in embryos (Fig. 3A, WT), while levels of SEC24D were comparable between the two (Fig. 3B, see WT). Interestingly, the levels of SEC24B and SEC24C were very low in wild-type yolk sacs (Fig. 3B, see WT), but collagen processing proceeded normally in this tissue (Fig. 3C, WT yolk sacs). This result suggests that both SEC24B and SEC24C are dispensable and that SEC24A and SEC24D are sufficient to export procollagen efficiently from the ER.

SEC24B is deficient in Sec24d KO yolk sacs

It is plausible that the insufficiency of both SEC24B and SEC24C exacerbates the SEC24D deficit, leading to the prominent ER phenotypes in the mutant yolk sacs. Levels of *Sec24a* transcripts in *Sec24d* KO yolk sacs were comparable to those in wild-type yolk sacs (Fig. 3A). Surprisingly, levels of SEC24C were recovered in mutant yolk sacs although there were significant individual variations (Fig. 3B and Fig. S1, compare SEC24C in embryos with that in yolk sacs), suggesting the presence of a compensatory mechanism(s). Levels of SEC24B were not restored or were only marginally restored in mutant yolk sacs. Thus, SEC24B seems to be invariably limiting and likely modulates the ER phenotypes in the mutant.

Intrigued by the individual variation in the compensatory expression of *Sec24c*, we were curious if such variation affected collagen processing in the mutants. When we compared collagen processing in 71a and 71g animals, we observed far lower levels of procollagen in the 71a animal (Fig. 3D). However, we did not observe any increase in the processing of procollagen. Interestingly, we occasionally observed a cellular accumulation of FN1 in *Sec24d* KO yolk sacs (Fig. S1C and D). This could be due to an occasional low expression of *Sec24c* (Fig. S1A). It remains to be determined why the 71g animal does not show such response. Perhaps the increased expression of *Sec24c* and the reduction in the levels of procollagen in the 71a animal are consequences of ER stress responses as the overexpression of COPII genes and the reduction of ER load are known to be outcomes of the unfolded protein response (UPR) of the ER (Hollien et al., 2009; Melville et al., 2011; Sudhakar et al., 2000).

We then evaluated the relative levels of SEC24 paralogs in human bone-related cell lysates (Fig. 3E). Interestingly, calvarial osteoblasts showed reduced levels of SEC24B and SEC24C, compared to femoral osteoblasts. It is important to note that the ossification of long bones occurs through chondrocytes and that of neurocranium occurs through calvarial osteoblasts (Berendsen and Olsen, 2015). Unfortunately, we were not able to obtain femoral (epiphyseal) chondrocytes. However, the two human bone cell lysates clearly show differential expression of *SEC24* paralogs. It is thus likely the low levels of SEC24B and especially SEC24C in calvarial osteoblasts could account for the severe skull phenotypes documented in SEC24D patients (Garbes et al., 2015). It remains to be seen whether epiphyseal chondrocytes exhibit low expression levels of *SEC24* paralogs, but if this were the case it could potentially account for the severe fragility of the lone bones in SEC24D patients.

Knock down (KD) of an individual SEC24 paralog has a minimal effect on collagen export

The analyses of the mouse tissues suggest that the absence of SEC24D leads to a mild to modest reduction in collagen processing in embryos. Interestingly, both SEC24B and SEC24C are dispensable for collagen processing as observed in wild-type yolk sacs. However, this does not necessarily mean that SEC24B and SEC24C do not contribute to the process. This is partly because the absence of SEC24B appears to contribute to the stronger block of procollagen processing in mutant yolk sacs. Thus, we decided to systematically test the involvement of SEC24 paralogs in collagen secretion.

To test for the role of SEC24s in collagen secretion, we knocked down the expression of *Sec24* paralogs using RNA interference (RNAi) in wild-type mouse embryonic fibroblasts

(MEFs). Here, we monitored collagen levels in the cell and in the culture medium. Our RNAi approach yielded about 70% depletion of SEC24s (Fig. S2). It should be noted that the proteolytic processing of the precursor forms of collagen is inefficient in cultured cells (Canty and Kadler, 2005) as the collagen processing proteases are diluted in the culture medium, resulting in the presence of procollagens in the culture medium. As a control of a secretory cargo, we also monitored FN1. We confirmed the FN1 band in immunoblots with FN1-specific RNAi (Fig. S3). We reasoned that knockdown (KD) of any SEC24 paralogs that are critical for ER export would result in an accumulation of secretory proteins in the ER and a reduction of the secretory proteins in the culture medium. We did not observe such effects with the KD of individual *Sec24s* (Fig. 4A and B). Consistent with this result, collagen did not accumulate in *Sec24d* KO MEFs (Fig. S4). These results suggest that SEC24 paralogs have a redundant function for ER export of collagen and FN1 in MEFs.

SEC24A and SEC24D play a major role in procollagen export in MEFs

We then knocked down the expression of two *Sec24* paralogs simultaneously (Fig. 4C-F and Fig. S5A and B). When we attempted to deplete two SEC24 paralogs together we noticed that SEC24D KD became ineffective for unknown reasons. Perhaps SEC24D siRNAs were outcompeted by other SEC24 siRNAs for the RNA-induced silencing complex (Koller et al., 2006). To circumvent this problem, we used *Sec24d* KO MEFs when SEC24D depletion is needed. Knocking down SEC24B/C did not affect collagen levels (Fig. 4C and D), which was consistent with the mouse tissue results (Fig. 3B WT). Interestingly, a simultaneous KD of SEC24A with any SEC24 paralog resulted in cellular accumulation of collagen (Fig. 4C-F). Similarly, a simultaneous KD of SEC24D with any SEC24 paralog resulted in cellular

accumulation of collagen (Fig. 4C-F). It is important to note that COL1A1 is mostly found in the ER even in the control cells (Fig. 6A, Scr), but when the ER export is blocked, the ER collagen signals increase (Fig. 6A, ABC). The levels of secreted collagen were not reduced (Fig. 4C-F). This modest collagen phenotype likely occurred because we could not inhibit a target gene expression completely with RNAi. It is worth reemphasizing that any double combination including either SEC24A or SEC24D led to collagen accumulation in the cell. These results underscore the importance of SEC24A and SEC24D as compared to SEC24B and SEC24C. In other words, the presence of any two SEC24s except for SEC24A/D is not sufficient for efficient procollagen export. In addition, although SEC24B and SEC24C depletion, alone or together, had no effect on collagen export, when SEC24B or SEC24C was depleted together with either SEC24A or SEC24D, collagen accumulated in the cell. Thus, SEC24B and SEC24C do contribute to collagen export in concert with other partners. In contrast, FN1 accumulated in the cell only when SEC24C/D were knocked down (Fig. 4C-F), suggesting that FN1 prefers either SEC24C or SEC24D.

When a double KD led to cellular accumulation of COL1A1 or FN1, it did not lead to a reduction of secreted protein levels. This likely reflects a modest defect. As a control, we tested whether our RNAi approach could allow us to block collagen secretion. A KD of three SEC24 paralogs resulted in relatively modest collagen phenotypes such as an increase in cellular collagen levels or a decrease in secreted collagen levels (Fig. 5A-D and Fig. S5C and D). Interestingly, in the case of FN1, a KD of SEC24A/B/C or SEC24A/B/D did not lead to an increase in cellular FN1 levels, reinforcing the idea that SEC24C or SEC24D alone can support an efficient ER export of FN1.

A strong secretion block was achieved when the expression of all SEC24 paralogs was reduced (Fig. 5E and F and Fig. S5E). The levels of *Col1a1* mRNAs were not increased under the condition (Fig. S5F), indicating that the cellular collagen accumulation is not the consequence of an increased expression of *Col1a1* mRNAs. Consistent with this collagen secretion phenotype, intracellular COL1A1 was found in the ER (Fig. 6A and B) and the ER cisternae were enlarged drastically under this condition (Fig. 6C). Taken together, our data show that while SEC24A and SEC24D play a major role in ER export of procollagen in MEFs, SEC24B and SEC24C also contribute to the process, particularly when SEC24A and/or SEC24D are lacking. In the case of FN1, SEC24C and SEC24D act on FN1 redundantly.

DISCUSSION

Considering the similarities and differences in primary amino acid sequences and cargo binding sites of SEC24s, it is evident how SEC24 paralogs can have both distinct and overlapping cargo preferences. For example, VANGL2 is recognized preferably by SEC24B (Merte et al., 2010), SEC22 SNARE by SEC24A or SEC24B (Mancias and Goldberg, 2007), STX5 by SEC24C or SEC24D (Mancias and Goldberg, 2008), and p24 and ERGIC53 by any of SEC24s (Adolf et al., 2019; Ma et al., 2017). Here we showed that FN1 is favored by either SEC24C or SEC24D (Fig. 5A-D). However, procollagen is unique in that it can utilize SEC24A/D (including SEC24A/C/D), SEC24A/B/C, or SEC24B/C/D for ER export, suggesting that procollagen needs multiple SEC24 paralogs for efficient ER exit. As the IxM binding pocket of SEC24D is implicated in the SEC24D disease and this pocket is not available in SEC24A/B (Garbes et al., 2015; Mancias and Goldberg, 2008), SEC24A and SEC24B likely use a different cargo binding pocket. It is possible that procollagen needs two different cargo adaptors that are recognized by at least two different SEC24 paralogs because it is unusually long. Alternatively, procollagen could utilize one cargo adaptor that has two export signals recognized by two SEC24 paralogs. It is also possible that one of the two SEC24s recognizes a procollagen cargo adaptor and the other recognizes a molecule that should be co-packaged with procollagen. The exact mechanism remains to be determined.

Although the expression of *Sec24b* and *Sec24c* was very low, the ER was not distended in the wild-type yolk sac (Fig. 1D). In addition, the cells of the head and the tail did not show distended ER in the mutants. Furthermore, we did not observe a severe difference in the levels of secreted or intracellular collagen between wild-type and *Sec24d* KO MEFs (Fig. S4). These observations demonstrate the redundancy of the ER export system for procollagen.

In our *Sec24d* null mutants, we observed phenotypes arising from an ER export block such as a procollagen processing defect and enlarged ER cisternae. Interestingly, the collagen processing defect was more obvious in the yolk sac than in the embryo of the *Sec24d* mutants. Likewise, ER cisternae were more distended in the yolk sac than in the fibroblasts of the head or in the tail of the mutants. We reasoned that this tissue dependency was due to variable expression levels of another component of the ER export system. If the ER distension was solely driven by the lack of SEC24D alone, we would have also observed such ER distension in the head and the tail. Thus, it was evident that SEC24D alone is not responsible for the ER phenotypes. We suspected a second deficiency in the ER export system within the yolk sac.

Wild-type yolk sacs expressed very low levels of SEC24B and SEC24C, which indicates that SEC24B and SEC24C are dispensable for the normal functions in the yolk sac. One of the functions of the yolk sac is to secrete collagens to provide fetal membranes with resistance to rupture (Canty and Kadler, 2005; Dobreva et al., 2010; Mayer et al., 1998). The processing of procollagen was quite efficient in wild-type yolk sacs. Thus, it appears that SEC24A and SEC24D can handle the task of exporting procollagens and other cargo molecules from the ER of the yolk sac with high efficiency. Interestingly, compared to wild-type yolk sacs where only *Sec24a* and *Sec24d* are expressed, *Sec24d* KO mutant yolk sacs upregulate expression of *Sec24c*, which allows us to compare the functions of SEC24C and SEC24D for collagen secretion. Apparently, SEC24C cannot compensate for the loss of SEC24D, demonstrating the importance of SEC24D over SEC24C in collagen secretion. In addition, this result suggests that SEC24B is the tissue-specific factor whose absence contributed to the prominent collagen phenotypes in the yolk sacs of the *Sec24d* mutants. In the case of human calvarial osteoblasts, SEC24C seems to be the tissue-specific factor (Fig. 3E).

In cultured cells, the depletion of individual SEC24 paralogs did not inhibit collagen secretion. Any double or a triple SEC24 KD all resulted in a collagen phenotype except for the SEC24B/C double KD. These *in vitro* experiments allowed us to recognize the importance of SEC24A and SEC24D in collagen secretion, which is consistent with the expression pattern of *Sec24a* and *Sec24d* in wild-type yolk sacs (Fig. 3). Importantly, the depletion of either SEC24B or SEC24C together with SEC24A or SEC24D resulted in cellular collagen accumulation. Thus, we propose that SEC24A and SEC24D can be the major players required for procollagen export from the ER at least in MEFs and SEC24B and SEC24C also contribute to the process. This is unexpected because we initially thought that SEC24C and SEC24D would be the major players and that procollagen would behave just like FN1 in our KD experiments. It remains to be determined how multiple SEC24 paralogs work together to export procollagen from the ER.

As ER-to-Golgi SNAREs are differentially packaged by SEC24A/B and SEC24C/D into COPII vesicles (Mancias and Goldberg, 2008; Tang et al., 1999), a simultaneous depletion of two SEC24 paralogs can block the packaging of the SNAREs, which can inhibit procollagen export indirectly. For example, SEC24A/B packages the R-SNARE SEC22B and SEC24C/D packages the Q-SNARE complex (STX5/Sed5p, membrin/Bos1p/GS27 and BET1) into COPII vesicles (Adolf et al., 2019; Adolf et al., 2016; Mancias and Goldberg, 2008). Thus, a depletion of SEC24C/D or a depletion of SEC24A/B could block procollagen export indirectly because such depletion would block the packaging of the SNAREs into COPII vesicles. However, other combinations (e.g., a depletion of SEC24A/D or that of SEC24B/D) would not be expected to interfere with the packaging of the SNAREs into COPII vesicles. In addition, under our *in vitro* conditions, the depletion is not complete. Thus, such indirect effects are unlikely. In fact, a KD of SEC24A/B did not lead to a cellular accumulation of FN1 (Fig. 4C and D).

The vast majority of yolk sacs of *Sec23a* KO mutants are broken probably due to a severe collagen secretion block in the mutant yolk sacs (Zhu et al., 2015). We have not observed any broken yolk sacs in our mutants. Perhaps the secretion block in our mutant yolks sacs is not as severe as that in the *Sec23a* mutant because SEC24A and SEC24C can contribute to collagen secretion to a certain degree. Alternately, the yolk sac breakage may also involve other secretory proteins that are secreted normally in *Sec24d* KO yolk sacs. *Sec23a* KO mutants also present with reopening of the closed neural tube (Zhu et al., 2015). Such phenotype was not observed in our mutants, nor in the previous work describing *Sec24d* KO mutants (Baines et al., 2013). This reopening was caused by a collagen secretion defect in skin fibroblasts, which likely compromises the tensile strength of the skin tissue. We observed only a modest processing defect of collagen in embryo extracts (Fig. 1B). In addition, the ER of the head cells was not distended in the mutants (Fig. 1D). Thus, we do not expect a reduction in the tensile strength of the skin tissue of our mutants. Together, our work demonstrates that the unique tissue-specific consequences of *Sec24d* KO result from the variable presence of other SEC24 paralogs, and that SEC24 paralogs cooperate in a tissue-specific and cargo-specific manner to facilitate ER export of secretory proteins.

MATERIALS AND METHODS

Ethics Statement

All animal care and use complied with the Principles of Laboratory and Animal Care established by the National Society for Medical Research. The Institutional Animal Care and Use Committee (IACUC) of the Iowa State University approved all animal protocols in this study under protocol number 19-061. For the immunohistochemical work, all mice were housed in an AAALAC International-accredited facility under IACUC approval (protocol #156-01-22D, Sanford Research, Sioux Falls, SD, USA).

Generation of *Sec24d* KO mice

ES cell clone RRR785 was obtained from the International Gene Trap Consortium (IGTC, Bay Genomics, San Francisco, CA), and was referred to as *Sec24d*^{gt2}. ES cell culture and microinjection, and recovering the mutant allele were performed as described previously (Baines et al., 2013). Mice from *Sec24d*^{gt2} were genotyped using a PCR. A PCR reaction including a common forward primer (In20F1) (Table S1) located upstream of the insertion site in intron 20 and a reverse primer located downstream of the insertion site (In20R1) in intron 20 produces a 715 bp product from the wild-type allele. A PCR reaction including primer In20F1 and a reverse primer V20 located in the gene trap vector produces a 558 bp product from the gene trap allele.

Timed Mating

Timed matings were performed by intercrossing *Sec24d* heterozygous mice. Copulation plugs were noted next morning and counted as day E0.5 of embryonic development. Embryos were harvested from E8.5–E13.5 for genotyping and E12.5 for the preparation of mouse embryonic fibroblasts, tissue extracts, and histology samples. Genotyping was performed on genomic DNA isolated from yolk sacs or embryos.

Cell culture and transfection

Wild-type and mutant mouse embryonic fibroblasts (MEFs) were obtained from wild-type and knockout mice, respectively. All cell lines were maintained in Gibco^{TM} high glucose DMEM supplied with 10% FBS (Cat. 11995065 and 16000044, Thermo Fisher Scientific, Waltham, MA). A knockdown of a target gene was achieved with transfecting cells with specific siRNA (Table S2, Horizon Discovery, Lafayette, CO) with Lipofectamine RNAiMAX reagent (Cat. 13778, Thermo fisher Scientific, Waltham, MA) according to the manufacturer's protocol. MEF cells were seeded one day prior to transfection. Fifty nano molar of siRNAs (Table S2) and Lipofectamine RNAiMAX were mixed and added to DMEM in the absence of FBS at day 0. Media were removed and replaced with complete DMEM media at the following morning. Cells and media were collected next day (24h). The lysates of human femoral osteoblasts and human calvarial osteoblasts were purchased from ScienCell Research Laboratorires (Cat. 4606 and 4656, Carlsbad, CA).

Immunoblotting and antibodies

Animal tissues were lysed in Triton X-100 buffer (150 mM NaCl, 50 mM Tris-HCl, 1% Triton™ X-100, 0.05% SDS, 1 mM EDTA). Cultured cells were lysed in a RIPA buffer (Cat. 9806s, Cell Signaling, Denvers, MA). Cellular extracts were resolved in a 9% SDS-polyacrylamide gel and transferred to PVDF membranes (Cat. IPVH00010, MilliporeSigma, Burlington, MA) through a wet transfer. Membranes were blocked in 5% skim milk in Tris-buffered saline with 0.1% Tween 20 (TBST) for 1 hour and then incubated with primary antibodies. The membranes were washed with TBST and then incubated secondary antibodies conjugated with horseradish peroxidase. Proteins were visualized with an ECL western blotting detection kit (GE Healthcare, Chicago, IL) through an Azure c600 gel imaging system and bands were quantified with an Azurespot software (Dublin, CA). Anti-SEC24A antibody (Cat. 15958-1-AP) and Anti-fibronectin 1 antibody (15613-1-AP) were purchased from Proteintech (Rosemont, IL). Anti-SEC24B antibody (A304-876A), anti-SEC24C antibody (A304-759A) and anti-GAPDH antibody (A300-639A) were purchased from Bethyl Laboratories (Montgomery, TX). Anti-type I collagen α1 antibody (LF68, ENH018-FP) was purchased from Kerafast Inc.(Boston, MA). For immunohistochemistry, rabbit polyclonal anti-collagen I (203002, MD Bioproducts, Oakdale, MN). Anti- α-tubulin antibody (sc-8035) was purchased form Santa Cruz Biotechnology (Dallas, TX). Anti-SEC24D antibody (#3151) and anti-ribophorin I antibody are gifts from Randy Schekman at UC Berkeley. Anti-mouse PDI antibody (ADI-SPA-891) was purchased from Enzolifesciences (Farmingdale, NY).

Immunofluorescence and confocal imaging

Cells were seeded on a coverslip and fixed in 4% paraformaldehyde then permeabilized by incubation with 0.1% Triton™ X-100 (Fisher Scientific, Waltham, MA). After permeabilization,

the seeded coverslip was incubated with primary antibodies for 2 h at RT and followed by 1.5 h of a secondary antibody incubation. Mounting medium Mowiol/DAPI/PPD (MilliporeSigma, Burlington, MA) was applied when the coverslip was centered on slides. Anti-human procollagen type 1 antibody (LF68, ENH018) was purchased from Kerafast Inc. (Boston, MA) and anti-PDI antibody (ADI-SPA-891) was purchased from Enzo Life Sciences (Farmingdale, NY). Confocal images were taken with a Leica SP5 X (Exton, PA) confocal microscope at the Roy J. Carver High Resolution Microscopy Facility in the Iowa State University.

Electron Microscopy

MEFs were seeded on a six-well plate and transfected with mouse SEC24s siRNA. Transfected MEFs were fixed in fixative solution (1% paraformaldehyde, 3% glutaraldehyde and 1M pH 7.2 cacodylate buffer) for 24-48 hours. Images were taken with a 200kV JEOL 2100 scanning/transmission electron microscope at the Roy J. Carver high resolution microscopy facility in Iowa State University.

Quantitative PCR

Cellular RNAs were extracted using a TRIzol™ reagent (Cat. 15596026, Thermo Fisher Scientific, Waltham, MA) according to the manufacturer protocol and complementary DNAs were generated using an AccuScript High Fidelity 1st Strand cDNA Synthesis kit (Agilent Technologies, Santa Clara, VA). A quantitative PCR was performed using a QuantStudio™ 3 Real-Time PCR system (Thermo Fisher Scientific, Waltham, MA) with an SYBR green supermix fluorescein (Cat. 1708880, Bio-Rad Laboratories, Hercules, CA) for detection. qPCR

primers for mouse collagen (*Col1a1*) (Yamazaki et al., 2005), *Sec24a* and *Gapdh* were obtained from PrimerBank and their sequence information is shown in Table S1.

ACKNOWLEDGEMENTS: The authors acknowledge Dr. Marit Nilsen-Hamilton (Iowa State University) for helping to obtain mouse embryonic fibroblasts. Research reported in this publication was supported by the National Institute of General Medical Sciences of the National Institutes of Health under award number R01GM110373, the Sanford Research Imaging Core within the Sanford Research Center for Pediatric Research (NIH P20GM103620), and the Sanford Research Molecular Pathology Core within the Sanford Research Center for Cancer Biology (NIH P20GM103548).

AUTHOR CONTRIBUTION: CLL and JK designed the study; SB and JK contributed to the construction of mutant mice, JC and JW prepared for mouse tissues, JC, JB, SO, JW collected IF data in mouse tissues; CLL collected the data; CLL and JK wrote the manuscript. All contributed to editing and reviewing the manuscript.

REFERENCES

Adams, E.J., X.W. Chen, K.S. O'Shea, and D. Ginsburg. 2014. Mammalian COPII coat component SEC24C is required for embryonic development in mice. *The Journal of biological chemistry*. 289:20858-20870.

Adolf, F., M. Rhiel, B. Hessling, Q. Gao, A. Hellwig, J. Bethune, and F.T. Wieland. 2019. Proteomic Profiling of Mammalian COPII and COPI Vesicles. *Cell Rep*. 26:250-265 e255.

Adolf, F., M. Rhiel, I. Reckmann, and F.T. Wieland. 2016. Sec24C/D-isoform-specific sorting of the preassembled ER-Golgi Q-SNARE complex. *Mol Biol Cell*. 27:2697-2707.

Baines, A.C., E.J. Adams, B. Zhang, and D. Ginsburg. 2013. Disruption of the Sec24d gene results in early embryonic lethality in the mouse. *PLoS One*. 8:e61114.

Berendsen, A.D., and B.R. Olsen. 2015. Bone development. *Bone*. 80:14-18.

Canty, E.G., and K.E. Kadler. 2005. Procollagen trafficking, processing and fibrillogenesis. *J Cell Sci*. 118:1341-1353.

Carvalho, R.L., L. Jonker, M.J. Goumans, J. Larsson, P. Bouwman, S. Karlsson, P.T. Dijke, H.M. Arthur, and C.L. Mummery. 2004. Defective paracrine signalling by TGFbeta in yolk sac vasculature of endoglin mutant mice: a paradigm for hereditary haemorrhagic telangiectasia. *Development*. 131:6237-6247.

Chen, X.W., H. Wang, K. Bajaj, P. Zhang, Z.X. Meng, D. Ma, Y. Bai, H.H. Liu, E. Adams, A. Baines, G. Yu, M.A. Sartor, B. Zhang, Z. Yi, J. Lin, S.G. Young, R. Schekman, and D. Ginsburg. 2013. SEC24A deficiency lowers plasma cholesterol through reduced PCSK9 secretion. *eLife*. 2:e00444.

Dobreva, M.P., P.N. Pereira, J. Deprest, and A. Zwijsen. 2010. On the origin of amniotic stem cells: of mice and men. *Int J Dev Biol*. 54:761-777.

Garbes, L., K. Kim, A. Riess, H. Hoyer-Kuhn, F. Beleggia, A. Bevot, M.J. Kim, Y.H. Huh, H.S. Kweon, R. Savarirayan, D. Amor, P.M. Kakadia, T. Lindig, K.O. Kagan, J. Becker, S.A. Boyadjiev, B. Wollnik, O. Semler, S.K. Bohlander, J. Kim, and C. Netzer. 2015. Mutations in SEC24D, encoding a component of the COPII machinery, cause a syndromic form of osteogenesis imperfecta. *Am J Hum Genet*. 96:432-439.

Hollien, J., J.H. Lin, H. Li, N. Stevens, P. Walter, and J.S. Weissman. 2009. Regulated Ire1-dependent decay of messenger RNAs in mammalian cells. *J Cell Biol*. 186:323-331.

Koller, E., S. Propp, H. Murray, W. Lima, B. Bhat, T.P. Prakash, C.R. Allerson, E.E. Swayze, E.G. Marcusson, and N.M. Dean. 2006. Competition for RISC binding predicts in vitro potency of siRNA. *Nucleic Acids Res*. 34:4467-4476.

Lu, C.L., and J. Kim. 2020. Consequences of mutations in the genes of the ER export machinery COPII in vertebrates. *Cell Stress Chaperones*. 25:199-209.

Ma, W., E. Goldberg, and J. Goldberg. 2017. ER retention is imposed by COPII protein sorting and attenuated by 4-phenylbutyrate. *eLife*. 6.

Mancias, J.D., and J. Goldberg. 2008. Structural basis of cargo membrane protein discrimination by the human COPII coat machinery. *EMBO J*. 27:2918-2928.

Mayer, U., E. Kohfeldt, and R. Timpl. 1998. Structural and genetic analysis of laminin-nidogen interaction. *Ann N Y Acad Sci*. 857:130-142.

McCaughey, J., and D.J. Stephens. 2018. COPII-dependent ER export in animal cells: adaptation and control for diverse cargo. *Histochem Cell Biol*. 150:119-131.

Melville, D.B., M. Montero-Balaguer, D.S. Levic, K. Bradley, J.R. Smith, A.K. Hatzopoulos, and E.W. Knapik. 2011. The feelgood mutation in zebrafish dysregulates COPII-dependent secretion of select extracellular matrix proteins in skeletal morphogenesis. *Dis Model Mech*. 4:763-776.

Merte, J., D. Jensen, K. Wright, S. Sarsfield, Y. Wang, R. Schekman, and D.D. Ginty. 2010. Sec24b selectively sorts Vangl2 to regulate planar cell polarity during neural tube closure. *Nat Cell Biol*. 12:41-46; sup pp 41-48.

Miller, E.A., T.H. Beilharz, P.N. Malkus, M.C. Lee, S. Hamamoto, L. Orci, and R. Schekman. 2003. Multiple cargo binding sites on the COPII subunit Sec24p ensure capture of diverse membrane proteins into transport vesicles. *Cell*. 114:497-509.

Mossessova, E., L.C. Bickford, and J. Goldberg. 2003. SNARE selectivity of the COPII coat. *Cell*. 114:483-495.

Ohisa, S., K. Inohaya, Y. Takano, and A. Kudo. 2010. sec24d encoding a component of COPII is essential for vertebra formation, revealed by the analysis of the medaka mutant, vbi. *Developmental biology*. 342:85-95.

Sarmah, S., A. Barrallo-Gimeno, D.B. Melville, J. Topczewski, L. Solnica-Krezel, and E.W. Knapik. 2010. Sec24D-dependent transport of extracellular matrix proteins is required for zebrafish skeletal morphogenesis. *PLoS One*. 5:e10367.

Shoulders, M.D., and R.T. Raines. 2009. Collagen structure and stability. *Annu Rev Biochem*. 78:929-958.

Sudhakar, A., A. Ramachandran, S. Ghosh, S.E. Hasnain, R.J. Kaufman, and K.V. Ramaiah. 2000. Phosphorylation of serine 51 in initiation factor 2 alpha (eIF2 alpha) promotes complex formation between eIF2 alpha(P) and eIF2B and causes inhibition in the guanine nucleotide exchange activity of eIF2B. *Biochemistry*. 39:12929-12938.

Tang, B.L., J. Kausalya, D.Y. Low, M.L. Lock, and W. Hong. 1999. A family of mammalian proteins homologous to yeast Sec24p. *Biochem Biophys Res Commun*. 258:679-684.

Wang, B., J.H. Joo, R. Mount, B.J.W. Teubner, A. Krenzer, A.L. Ward, V.P. Ichhaporia, E.J. Adams, R. Khoriaty, S.T. Peters, S.M. Pruett-Miller, S.S. Zakharenko, D. Ginsburg, and M. Kundu. 2018. The COPII cargo adapter SEC24C is essential for neuronal homeostasis. *J Clin Invest*. 128:3319-3332.

Yamazaki, K., H. Fukata, T. Adachi, H. Tainaka, M. Kohda, M. Yamazaki, K. Kojima, K. Chiba, C. Mori, and M. Komiyama. 2005. Association of increased type I collagen expression and relative stromal overgrowth in mouse epididymis neonatally exposed to diethylstilbestrol. *Mol Reprod Dev*. 72:291-298.

Zanetti, G., K.B. Pahuja, S. Studer, S. Shim, and R. Schekman. 2012. COPII and the regulation of protein sorting in mammals. *Nat Cell Biol*. 14:20-28.

Zhu, M., J. Tao, M.P. Vasievich, W. Wei, G. Zhu, R.N. Khoriaty, and B. Zhang. 2015. Neural tube opening and abnormal extraembryonic membrane development in SEC23A deficient mice. *Sci Rep*. 5:15471.

FIGURE LEGENDS

Figure 1. Tissue-dependent phenotypes in *Sec24d* KO tissues. (A) A schematic illustration of collagen processing. Extracts of embryos (B) and yolk sacs (C) were resolved and analyzed with immunoblotting. Asterisks, non-specific bands. Closed arrowheads, normal collagen species. Open arrowhead, abnormal collagen species. α-tubulin was used as a loading control. (D) Embryos and yolk sacs were processed for TEM. A part of the head, the tail and the yolk sac of wild-type and *Sec24d* KO mice are shown. ER cisternae were indicated by white arrowheads.

Figure 2. COL1A1 accumulates in yolk sac cells of *Sec24d* KO mutants. (A-H) Anti-COL1A immunoreactivity in WT (A-B, E-F) and *Sec24d*$^{gt2/gt2}$ mutant (C-D, G-H) head skin (A-D) and yolk sac (E-H). Embryo skin displayed similar immunoreactivity patterns in both genotypes. In the yolk sac, *Sec24d*$^{gt2/gt2}$ mutants had an apparent massive accumulation of COL1A1 in the cells lining the lumen (white arrowheads). FN1 expression patterns were similar between genotypes in both the embryo head skin (I-L) and in the yolk sac (M-P). Insets in the bottom right of G and H represent higher magnification images of the boxed regions. Scale bar in H inset is 20 μm for both insets. Scale bar in P is 50 μm for all other images.

Figure 3. SEC24B is deficient in the yolk sac of *Sec24d* KO mutants. (A) Levels of *Sec24a* mRNAs were measured with RT-qPCR and were normalized to those of *Gapdh* mRNAs. E, embryo; Y, yolk sac. (A) Student's t-test: WT, P*<0.005, n=4; *Sec24d* KO, P*<0.01, n=3. Error bars represent standard deviation. (B) SEC24B, SEC24C, and SEC24D were probed with immunoblotting using the extracts of wild-type (WT) and *Sec24d* KO (KO) mutant animals. E,

embryo; Y, yolk sac. Ribophorin I or GAPDH was used as a loading control. (C and D) COL1A1 was probed in the yolk sac extracts of WT (71c, 71d, and 71e) and *Sec24d* KO mutants (71a and 71g). Open arrowhead, abnormally processed collagen (see Fig 1C 92a animal). Ribophorin I was used as a loading control. (E) SEC24s were probed in lysates from human femoral osteoblasts (feO) and human calvarial osteoblasts (calO).

Figure 4. SEC24B and SEC24C have the least effect on collagen secretion. Wild-type (A-D) or *Sec24d* KO (E and F) MEFs were transfected with indicated siRNAs (50 nM) at day 0. The culture medium was replaced with fresh medium at day 1. Cells and a conditioned medium were harvested at day 2. Cell lysates and media were analyzed by immunoblotting (A, C and E). The levels of proteins in the lysates were normalized to those of α-tubulin and the levels of COL1A and FN1 in the medium were normalized to total protein amounts. In each experimental set, the levels of COL1A and FN1 were normalized to those in control (scrambled siRNA). Asterisks, nonspecific proteins. Scr, scrambled. Statistical significance was determined with Student's t-test. Error bars represent standard deviation. (B) A KD of *Sec24b* led to an increase of secreted collagen, which happened to coincide with the increased expression of *Sec24a* (Fig. S2). P*<0.05, n=4. (D) COL1A1: P*<0.05, P**<0.0005, n=3; FN1: P*<0.05, P**<0.005, $P^{\#}$<0.0005, n=3. (F) COL1A1: P*<0.05, P**<0.005, n=4; FN1: P*<0.05, n=3.

Figure 5. All SEC24s contribute to collagen secretion. Wild-type (A and B) or *Sec24d* KO (C-F) MEFs were treated and analyzed as described in the legend of Fig. 4. Asterisks, nonspecific proteins. Scr, scrambled. Statistical significance was determined with Student's t-test. Error bars

represent standard deviation. (B) P*<0.05, n=3. (D) COL1A1: P*<0.01, P**<0.005, P$^{\#}$<0.0001, n=4. FN1: P*<0.05, P**<0.0001, n=4, (F) P*<0.05, P**<0.0005, n=3.

Figure 6. Collagen accumulates in the ER in SEC24-depleted cells. *Sec24d* KO MEFs were transfected with indicated siRNAs (50 nM) at day 0. The culture medium was replaced with fresh medium at day 1. Cells were fixed at day 2 and processed for immunfluorescent labeling (A) or for electron microscopy (C). (A) Protein disulfide isomerase (PDI) was used as an ER marker. Scale bar, 20 μm. Inset, an enlarged image of the indicated region with a box. Arrowheads, a region of the ER that shows strong collagen signals. PDI signals were also stronger in the Sec24-depleted cells, reflecting an increase of the unfolded protein response of the ER. (B) Fluorescent signals (corrected total cell fluorescence) of collagen and PDI were quantified with ImageJ and collagen signals were normalized to PDI signals. Statistical significance was determined with Student's t-test. P*<0.0001, n=102 (Scr, Scrambled siRNA), n=104 (ABC, siRNAs for *Sec24a*, *Sec24b* and *Sec24c*). (C) Electron micrographs of *Sec24d* KO MEFs transfected with scrambled siRNA (Scr) or siRNAs for *Sec24a*, *Sec24b* and *Sec24c* (ABC). ER cisternae were indicated with arrowheads. Scare bar, 1 μm.

A

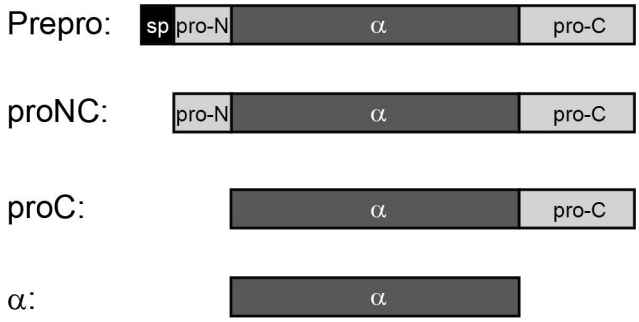
Prepro:
sp
pro-N
α
pro-C
proNC:
pro-N
α
pro-C
proC:
α
pro-C
α:
α

B

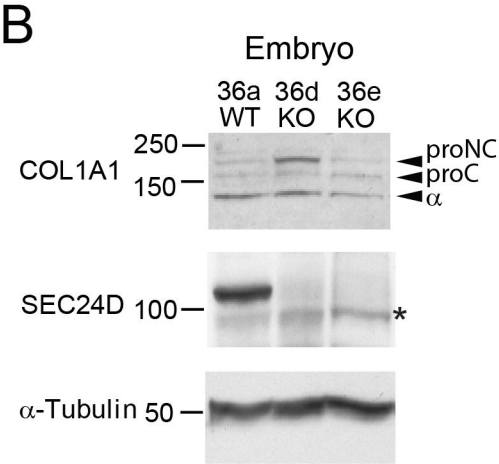
Embryo
36a WT
36d KO
36e KO
COL1A1
250
150
proNC
proC
α
SEC24D
100
*
α-Tubulin
50

C

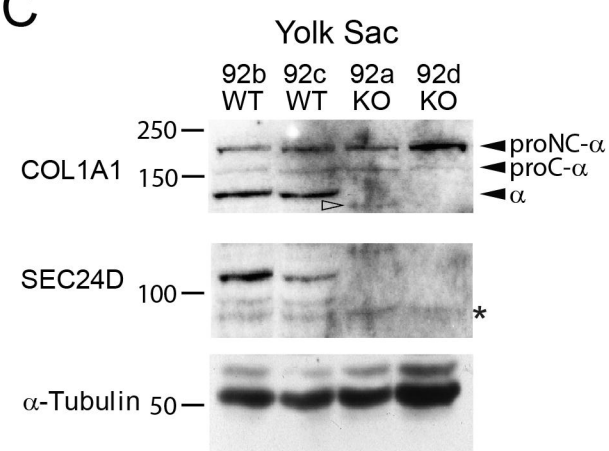
Yolk Sac
92b WT
92c WT
92a KO
92d KO
COL1A1
250
150
proNC-α
proC-α
α
SEC24D
100
*
α-Tubulin
50

D

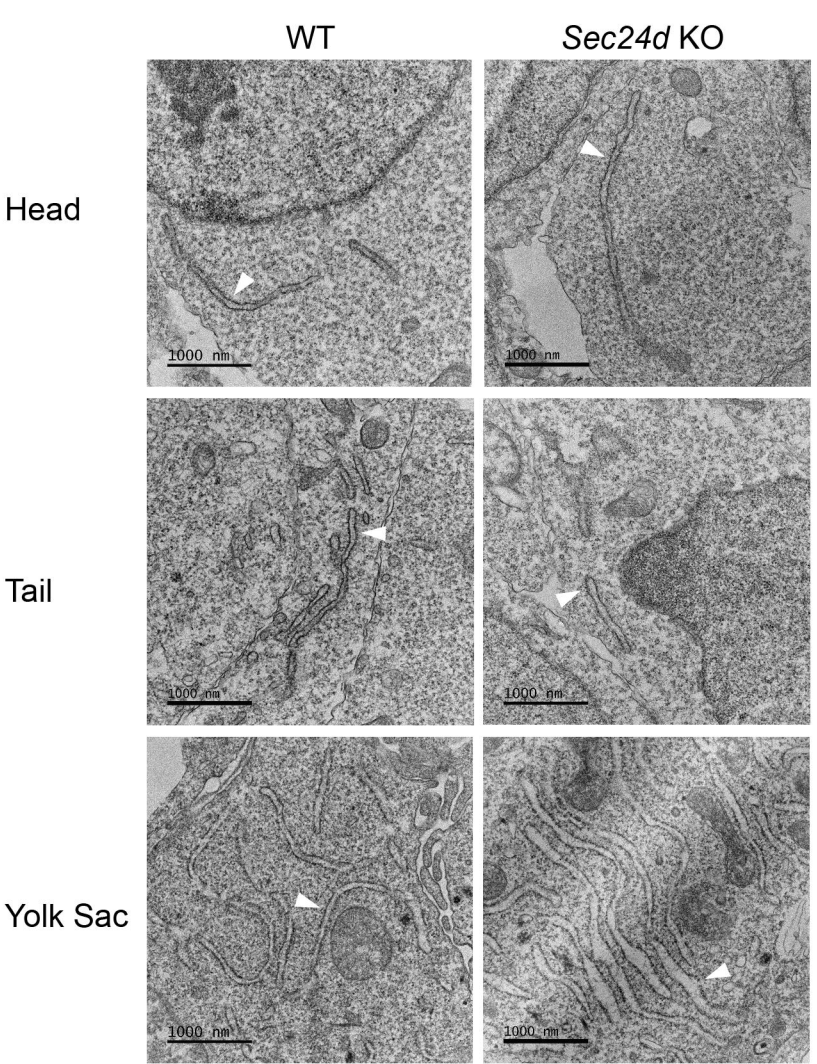
WT
Sec24d KO
Head
Tail
Yolk Sac
1000 nm

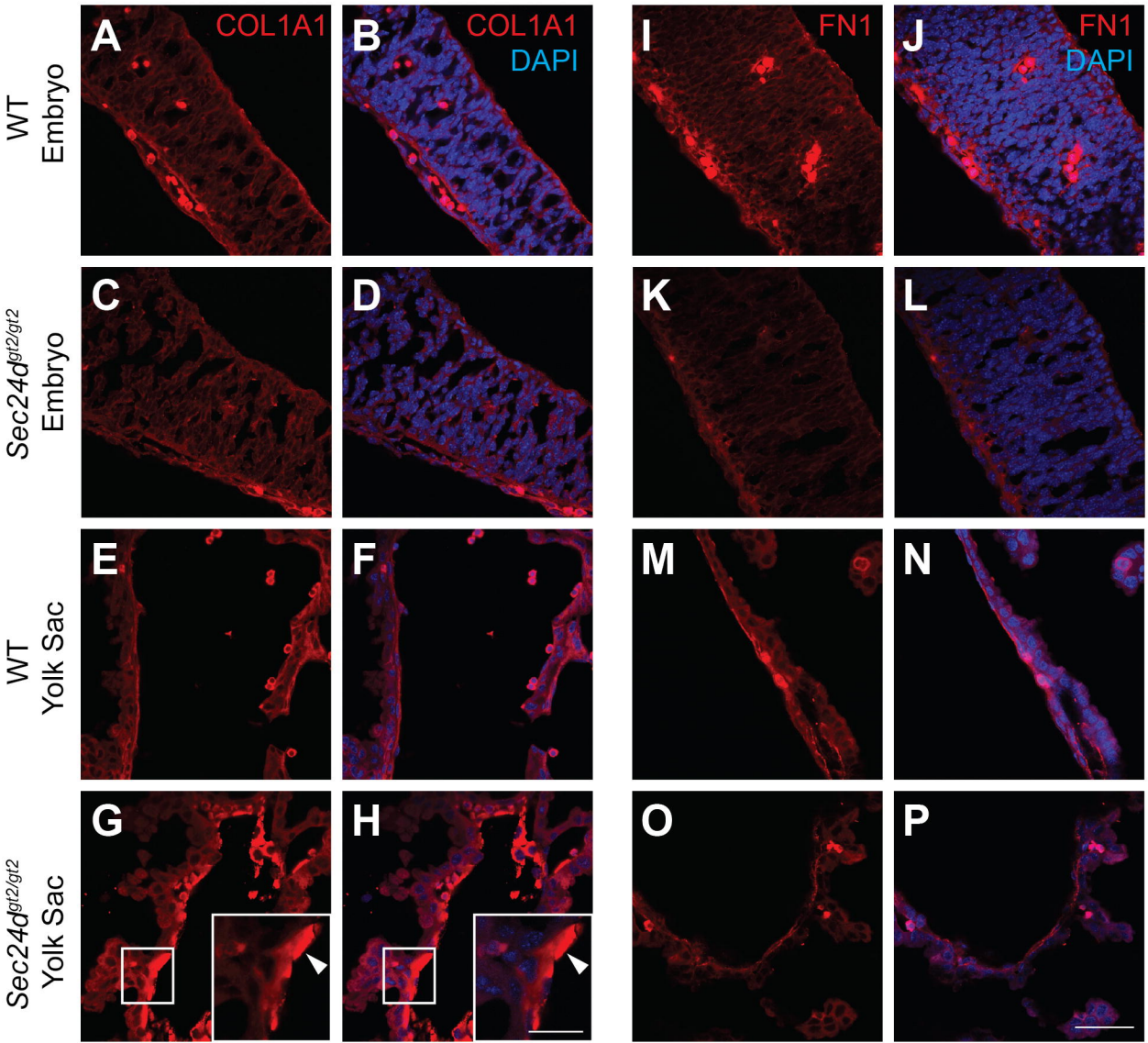
WT Embryo
Sec24d^gt2/gt2 Embryo
WT Yolk Sac
Sec24d^gt2/gt2 Yolk Sac
A
COL1A1
B
COL1A1
DAPI
I
FN1
J
FN1
DAPI
C
D
K
L
E
F
M
N
G
H
O
P

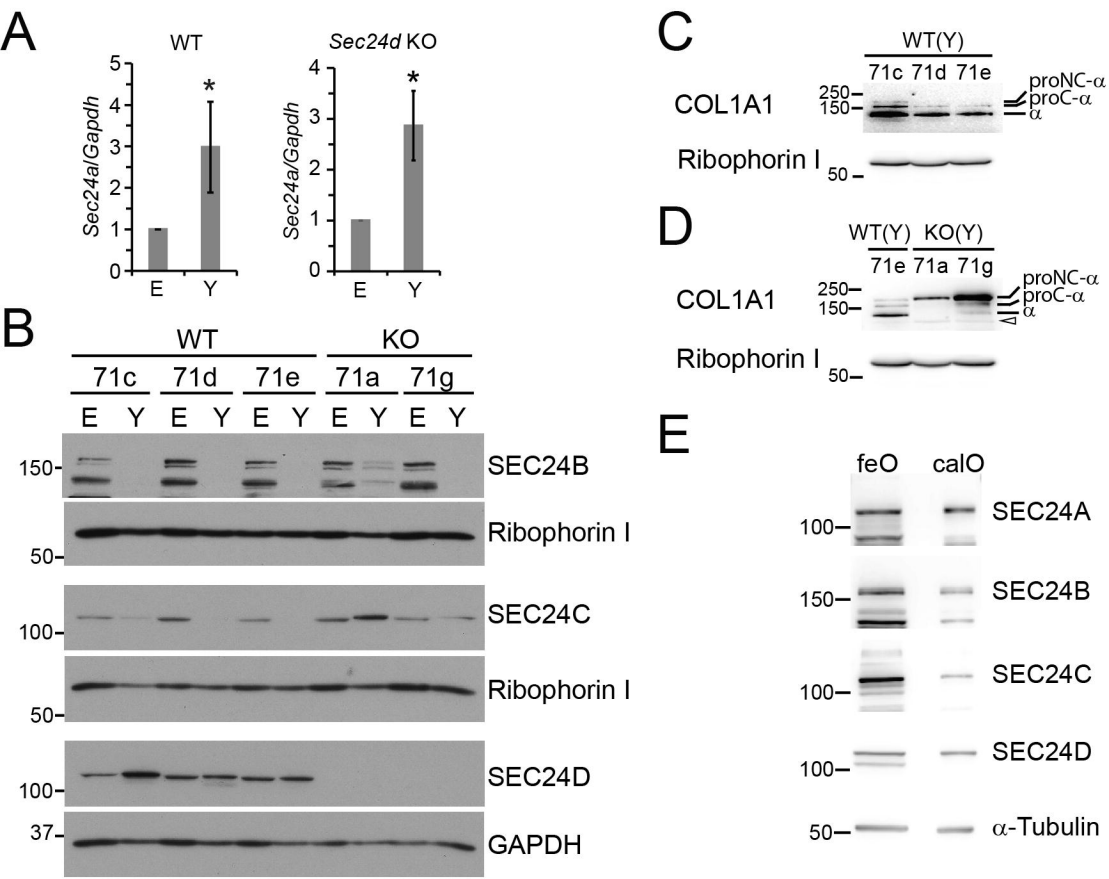
A
WT
Sec24d KO
Sec24a/Gapdh
Sec24a/Gapdh
E
Y
B
WT
KO
71c
71d
71e
71a
71g
E Y E Y E Y E Y E Y
150
SEC24B
Ribophorin I
50
100
SEC24C
Ribophorin I
50
SEC24D
100
37
GAPDH
C
WT(Y)
71c 71d 71e
COL1A1
250
150
proNC-α
proC-α
α
Ribophorin I
50
D
WT(Y) KO(Y)
71e 71a 71g
COL1A1
250
150
proNC-α
proC-α
α
Ribophorin I
50
E
feO
calO
100
SEC24A
150
SEC24B
100
SEC24C
100
SEC24D
50
α-Tubulin

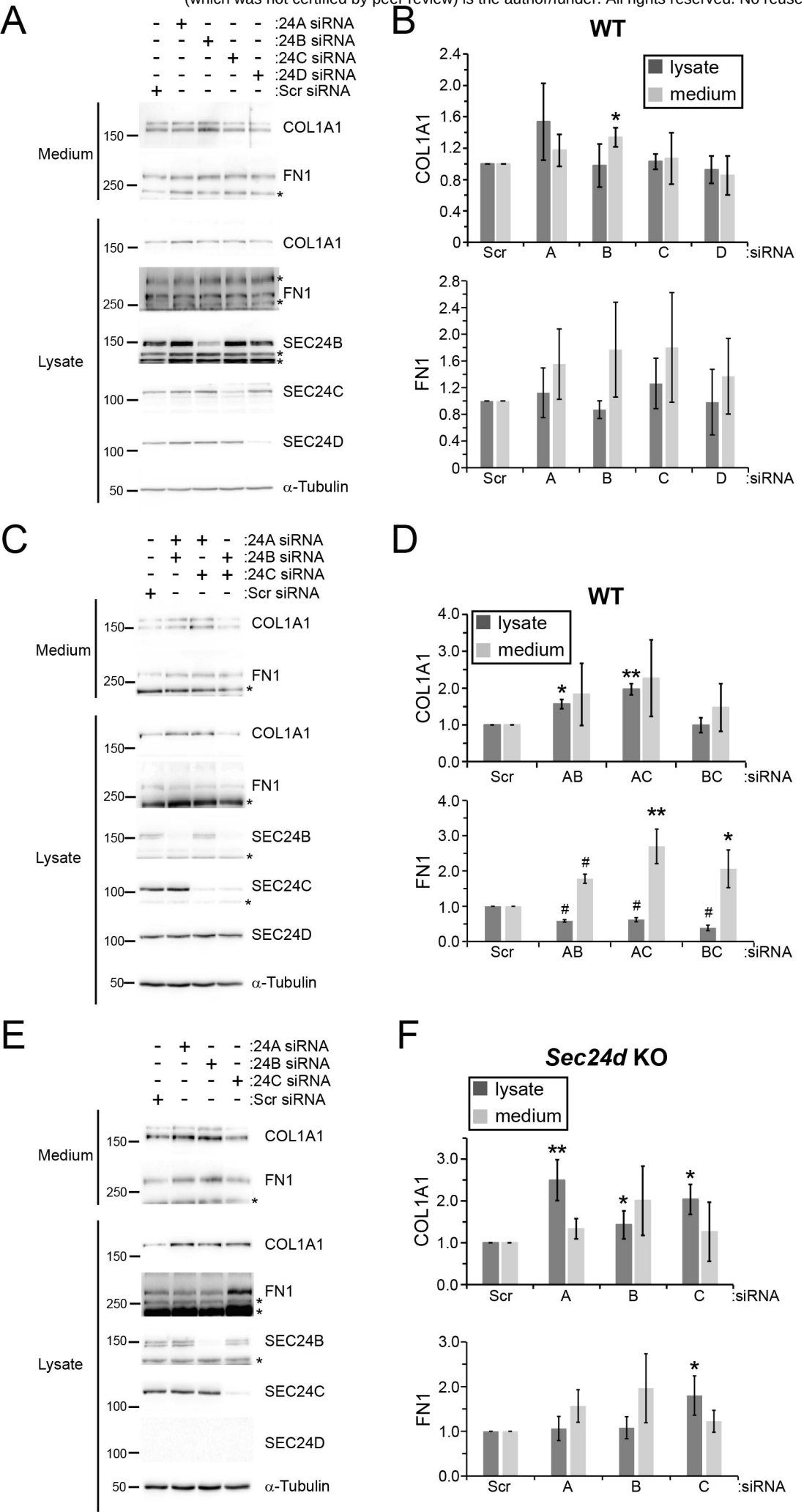

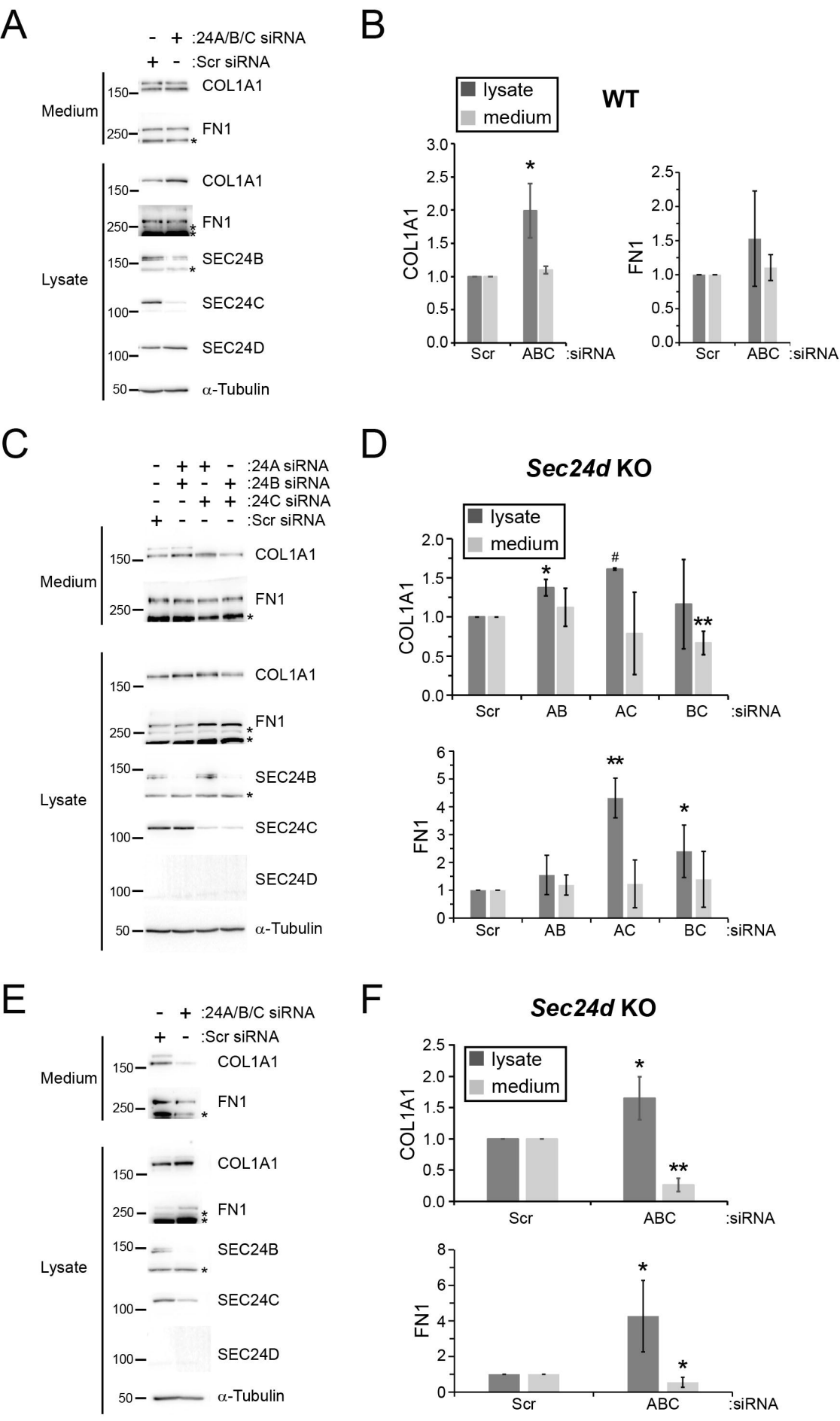
A
- + :24A/B/C siRNA
+ - :Scr siRNA
Medium
150
COL1A1
250
FN1
Lysate
150
COL1A1
250
FN1
150
SEC24B
100
SEC24C
100
SEC24D
50
α-Tubulin
B
lysate
medium
WT
COL1A1
FN1
Scr
ABC
:siRNA
C
- + + - :24A siRNA
- + - + :24B siRNA
- - + + :24C siRNA
+ - - - :Scr siRNA
Medium
COL1A1
FN1
Lysate
COL1A1
FN1
SEC24B
SEC24C
SEC24D
α-Tubulin
D
Sec24d KO
lysate
medium
COL1A1
FN1
Scr
AB
AC
BC
:siRNA
E
- + :24A/B/C siRNA
+ - :Scr siRNA
Medium
COL1A1
FN1
Lysate
COL1A1
FN1
SEC24B
SEC24C
SEC24D
α-Tubulin
F
Sec24d KO
lysate
medium
COL1A1
FN1
Scr
ABC
:siRNA

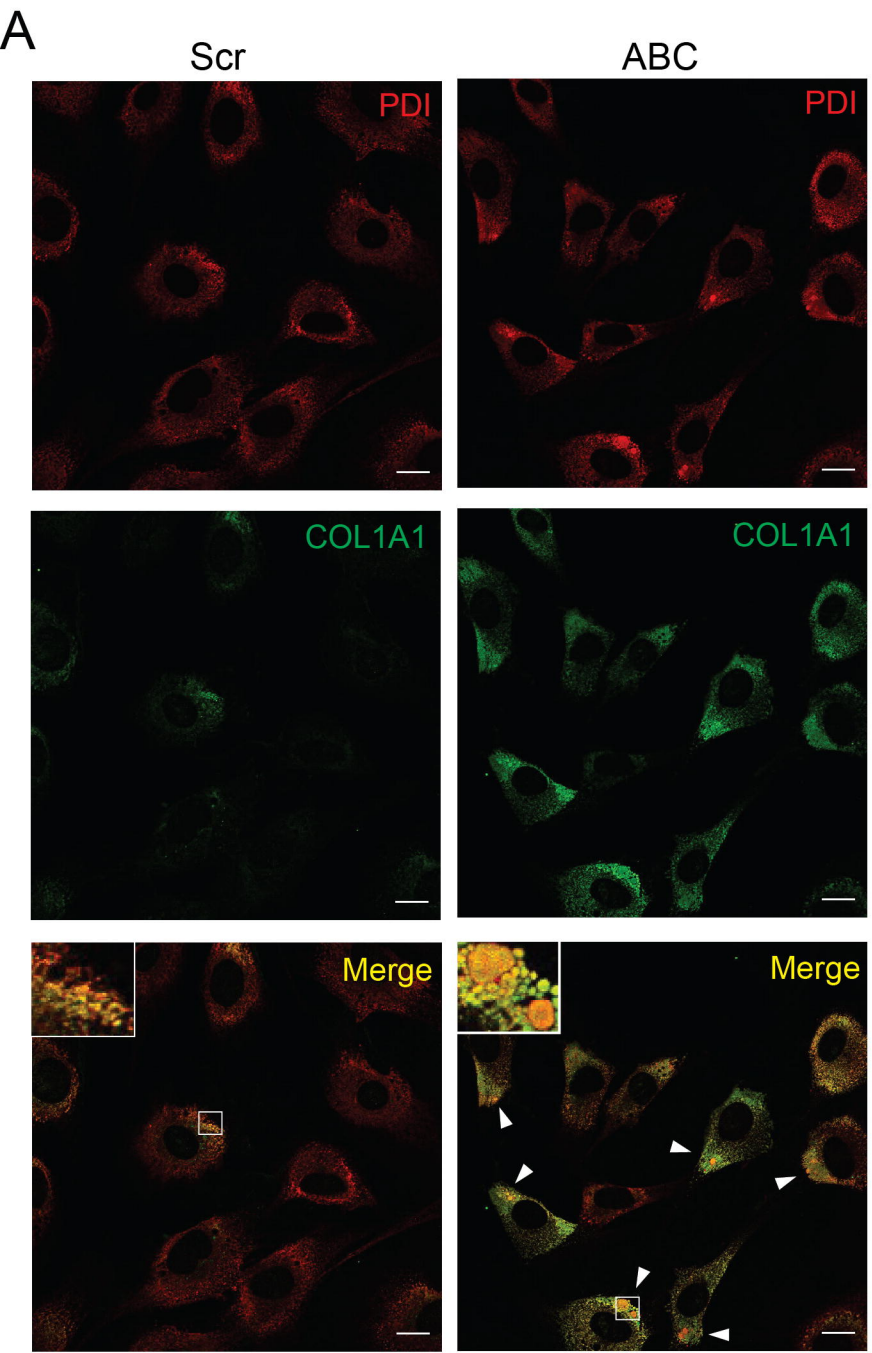
A
Scr
ABC
PDI
PDI
COL1A1
COL1A1
Merge
Merge

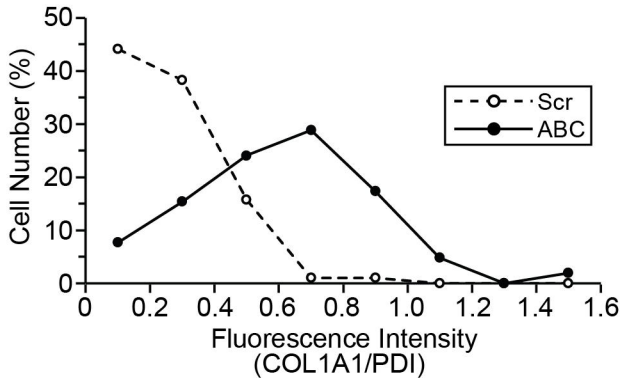
B
Cell Number (%)
50
40
30
20
10
0
0
0.2
0.4
0.6
0.8
1.0
1.2
1.4
1.6
Fluorescence Intensity
(COL1A1/PDI)
Scr
ABC

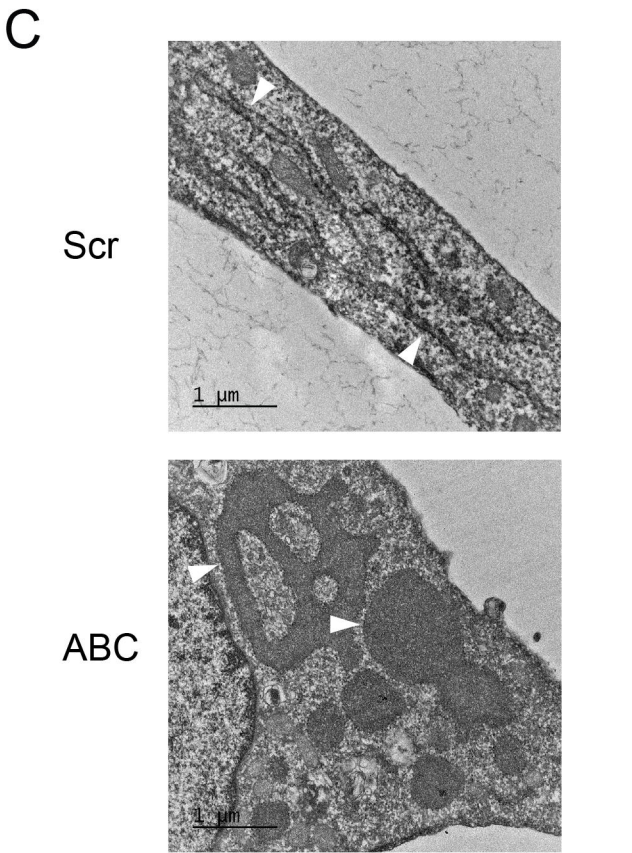
C
Scr
1 μm
ABC
1 μm